Supporting Information for
Original article

G protein-coupled receptor 35 attenuates nonalcoholic steatohepatitis by reprogramming cholesterol homeostasis in hepatocytes

Xiaoli Wei[a,†], Fan Yin[b,c,†], Miaomiao Wu[a,c,†], Qianqian Xie[c,d], Xueqin Zhao[c,d], Cheng Zhu[a], Ruiqian Xie[c,d], Chongqing Chen[c,d], Menghua Liu[c,d], Xueying Wang[a], Ruixue Ren[a], Guijie Kang[c,d], Chenwen Zhu[a], Jingjing Cong[c,d], Hua Wang[a,d,*], Xuefu Wang[c,d,*]

[a]*Department of Oncology, the First Affiliated Hospital of Anhui Medical University, Hefei 230036, China*

[b]*Department of Pharmacy, Huainan First People's Hospital, the First Affiliated Hospital of Anhui University of Science and Technology, Huainan 232001, China*

[c]*School of Pharmacy, Anhui Medical University, Hefei 230032, China*

[d]*Inflammation and Immune Mediated Diseases Laboratory of Anhui Province, Anhui Medical University, Hefei 230032, China*

Received 28 May 2022; received in revised form 8 August 2022; accepted 18 August 2022

[*]Corresponding authors.

E-mail addresses: wangxuefu@ahmu.edu.cn (Xuefu Wang),wanghua@ahmu.edu.cn (Hua Wang).

[†]These authors made equal contributions to this work.

1. Supporting tables

Table S1 List primers for q-PCR.

Gene (Mouse)	Forward primer (5′–3′)	Reverse primer (5′–3′)
β-Actin	GGCTGTATTCCCCTCCATCG	CCAGTTGGTAACAATGCCATGT
Gpr35	CAATACCTGTGCTGCCCGAGAC	GTGGCTGGCTTGGACGCTTC
Cyp27a1	AGACCATCGGCACCTTTCCTGAG	GCACCACACCAGTCACTTCCTTG
Cyp7a1	GTGATGTTTGAAGCCGGATATC	TTTATGTGCGGTCTTGAACAAG
Cyp8b1	TCCCCTATCTCTCAGTACACAT	ACTTGTAGAAGTCCACTTTCCG
Cyp7b1	AACCCTTTCCAGTACCAGTATG	GTGAACGTCTTCATTAAGGTCG
Acat2	CGCTGCTGCTGTGGTCCTTATG	GCTTGCTTTATGGCTGGAATTGGTC
Acc	GAAGCCACAGTGAAATCTCG	GATGGTTTGGCCTTTCACAT
Pparα	AACATCGAGTGTCGAATATGTGG	CCGAATAGTTCGCCGAAAGAA
Cpt1α	AGCCAGACTCCTCAGCAGCAG	CACCATAGCCGTCATCAGCAACC
Tnfα	GAGAGAAAGTGAGTGCGTCCCTTG	GGCAACAGCACCGCAGTACC
Il6	CTTCTTGGGACTGATGCTGGTGAC	AGGTCTGTTGGGAGTGGTATCCTC
Il1β	TCGCAGCAGCACATCAACAAGAG	AGGTCCACGGGAAAGACACAGG
Srebp1c	AACGTCACTTCCAGCTAGAC	CCACTAAGGTGCCTACAGAGC
Abcg5	CATTGAAAGAGCACGATACCTG	AGATTCTGAACGAGACGCATAA
Abcg8	GGACAAATTTGGATAAATGGGC	GATTACGTCTTCCACCCGTTT
Abca1	CCTCAGAGAAAACAGAAAACCG	CTTTGCTATGATCTGCACGTAC
Hmgcr	GGTGCAAAGTTCCTTAGTGATG	GAATAGACACACCACGTTCATG
Ldlr	CAGAAGTCGACACTGTACTGAC	AAGATGGACAGGAACCTCATAC
Srb1	AACATCACCTTCAATGACAACG	ACCAAGATGTTAGGCAGTACAA
Npc1l1	CTGGCTGGCTCTCATCATCATCTTC	AGCCTGCTGTCTTGTTCTTGTTCC
Ntcp	CATGGAGTTCAGCAAGATCAAG	CTCAATGCTGGTCAGATGAAAG
Bat	GGTGTAGAGTTTCTCCTGAGAC	CAATCTCTGCTCCAATGCATAC
Bal	CCAAAACGATTGCTAAGAAGGT	CAATGTCAGCAGTGTTGTTGTA
Hnf4a	TGAGGAAGAACCACATGTACTC	GTAACGACACTGGTTCCTCTTA
Osta	CTCTGTTCCAGGTGCTTGTCATCC	ATGTGGCAGTTCATCACTTGAGACC
Ostb	GGAACTGCTGGAAGAAATGCTTTGG	CCTTCTCAGGAGGAACATGCTTGTC
Abcb11	GTGTCTACTTCATGCTTGTGAC	GAGACTTAGATCGTTGACGGAT
Abcb4	TGATAGCTCACCGATTGTCTAC	CGAGTCTGAAGTAGATCCCTTC
Ibabp	TTCAAGATCATCACAGAGGTCC	CATGGTCTGCATTTCACATTCT
Asbt	GCGACATGGACCTCAGTGTTAGC	GTTCCCGAGTCAACCCACATCTTG

Table S2 List for primary antibodies.

Antibodies	Sources	Identifier
Anti-beta-Actin	Cell Signaling Technology	Cat# 3700
Anti-Fatty Acid Synthase	Cell Signaling Technology	Cat# 3180
Anti-AKT	Cell Signaling Technology	Cat# 9272
Anti-phospho-Akt	Cell Signaling Technology	Cat# 4060
Anti-p44/42 MAPK (Erk1/2)	Cell Signaling Technology	Cat# 4695
Anti-phospho-p44/42 MAPK (Erk1/2)	Cell Signaling Technology	Cat# 4370
Anti-p38 MAPK	Cell Signaling Technology	Cat# 9212
Anti-phospho-p38 MAPK	Cell Signaling Technology	Cat# 9216
Anti-SAPK/JNK	Cell Signaling Technology	Cat# 9252
Anti-phospho-SAPK/JNK	Cell Signaling Technology	Cat# 9251
Anti-IRE1α	Cell Signaling Technology	Cat# 3294
Anti-phospho-ERK5	Cell Signaling Technology	Cat# 3371
Anti-CREB	Cell Signaling Technology	Cat# 9197
Anti-phospho-CREB	Cell Signaling Technology	Cat# 9198
Anti-ERK5	Abcam	Cat# ab40809
Anti-GRP78	Abcam	Cat# ab108613
Anti-ATF6	Abcam	Cat# ab227830
Anti-Cpt1α	Abcam	Cat# ab234111
Anti-STARD4	Abcam	Cat# ab202060
Anti-ACAT2	Abcam	Cat# ab191431
Anti-SR-BI	Abcam	Cat# ab217318
Anti-CYP27A1	Abcam	Cat# ab126785
Anti-SREBP1	Abcam	Cat# ab28481
Anti-SREBP2	Santa Cruz Biotechnology	Cat# sc-13552
Anti-CYP8B1	Santa Cruz Biotechnology	Cat# sc-101387
Anti-GPR35	Novus Biologicals	Cat# NBP2-24640
Anti-CYP7A1	Affinity Biosciences	Cat# DF2612
Anti-CYP7B1	Proteintech	Cat# 24889-1-AP
Anti-CHOP	Proteintech	Cat# 15204-1-AP
Anti-PERK	Proteintech	Cat# 20582-1-AP

2. Supporting figures

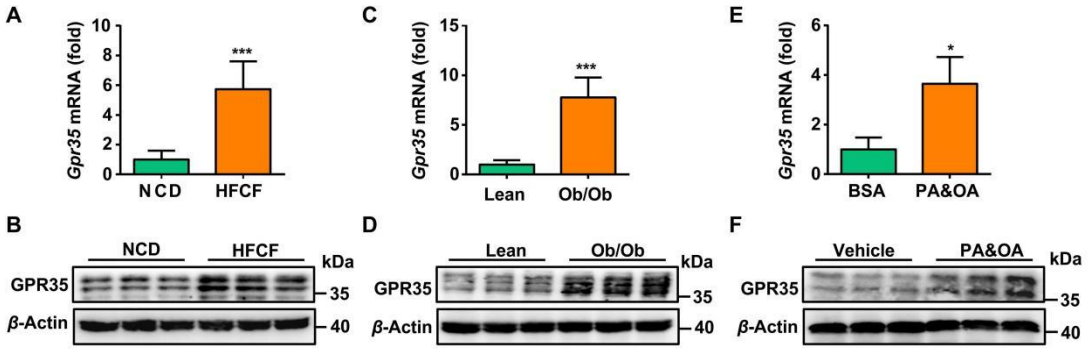

Figure S1 GPR35 expression in hepatocytes is increased significantly in NAFLD. (A) Relative mRNA expression and (B) representative Western blot of GPR35 in hepatocytes isolated from WT mice fed a NCD or HFCF for 16 weeks (n = 6). (C) Relative mRNA expression and (D) representative Western blot of GPR35 in hepatocytes isolated from WT and *ob*/*ob* mice (n = 6). (E) Relative mRNA expression and (F) representative western blot of GPR35 in primary hepatocytes treated with PA&OA or BSA for 24 h (n = 3). The mRNA expression of genes was normalized to that of β-actin. Data are the mean ± SD; *P < 0.05, **P < 0.01, ***P < 0.001. PA, palmitic acid; OA, oleic acid.

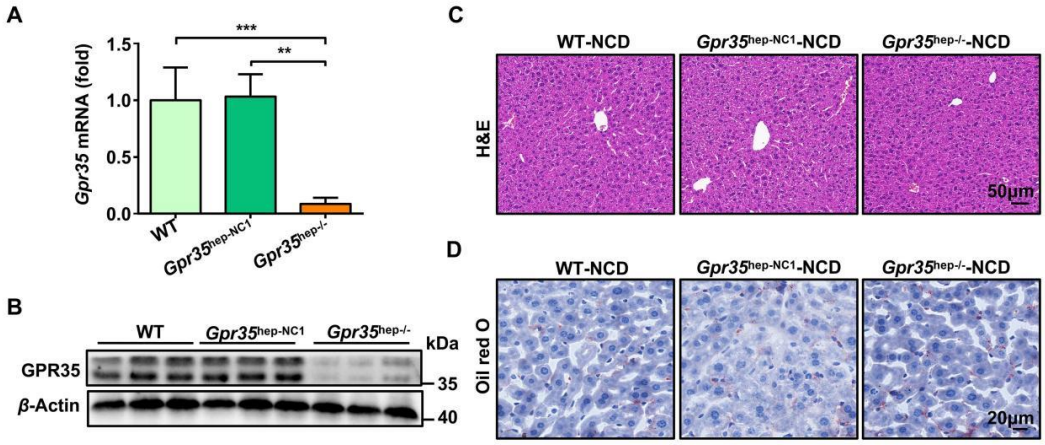

Figure S2 GPR35 knockout in hepatocytes (n = 3). C57BL/6J mice were injected (i.v.) with AAV8-TBG-SaCas9-2A-EGFP-U6-sgRNA (NC) or AAV8-TBG-SaCas9-2A-EGFP-U6-sgRNA (*Gpr35*). Control (*Gpr35*$^{hep\text{-}NC1}$) and hepatocyte *Gpr35*-knockout (*Gpr35*$^{hep-/-}$) mice were generated 1 week later. (A) Relative mRNA expression of *Gpr35* in primary hepatocytes. The mRNA expression of genes was normalized to that of *β*-actin. (B) Representative western blot of GPR35 in primary hepatocytes. (C) H&E staining of liver tissue sections. Scale bar, 50 μm. (D) Oil Red O staining of liver tissue sections. Scale bar, 20 μm. Data are the mean ± SD; $^{**}P < 0.01$, $^{***}P < 0.001$.

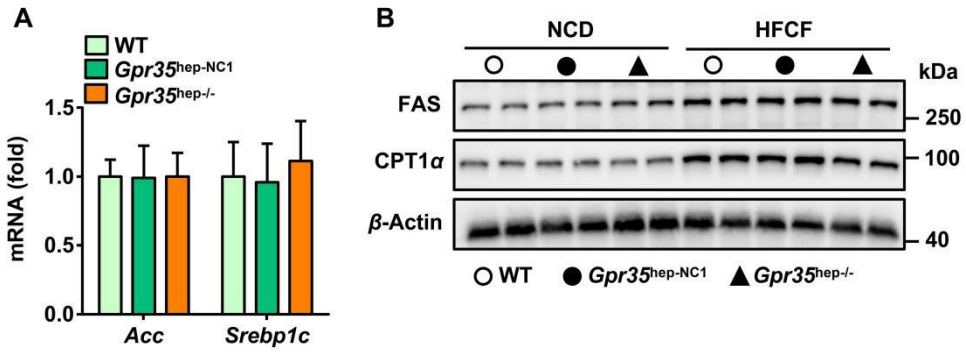

Figure S3 Loss of GPR35 in hepatocytes reduces the expression of the genes involved in fatty acid oxidation but not *de novo* lipogenesis in the livers of mice fed a HFCF diet (n = 10). C57BL/6J mice were injected (i.v.) with AAV8-TBG-SaCas9-2A-EGFP-U6-sgRNA (NC) or AAV8-TBG-SaCas9-2A-EGFP-U6-sgRNA (*Gpr35*) to generate control ($Gpr35^{hep\text{-}NC1}$) mice and hepatocyte *Gpr35*-knockout ($Gpr35^{hep-/-}$) mice, which were then fed the NCD or HFCF diet for 16 weeks. (A) Relative mRNA expression of *Acc* and *Srebp1c* in the livers of mice fed the HFCF. The mRNA expression of genes was normalized to that of β-actin. (B) Representative Western blot of FAS and CPT1α in the livers of mice fed the NCD or HFCF diet. Data are the mean ± SD.

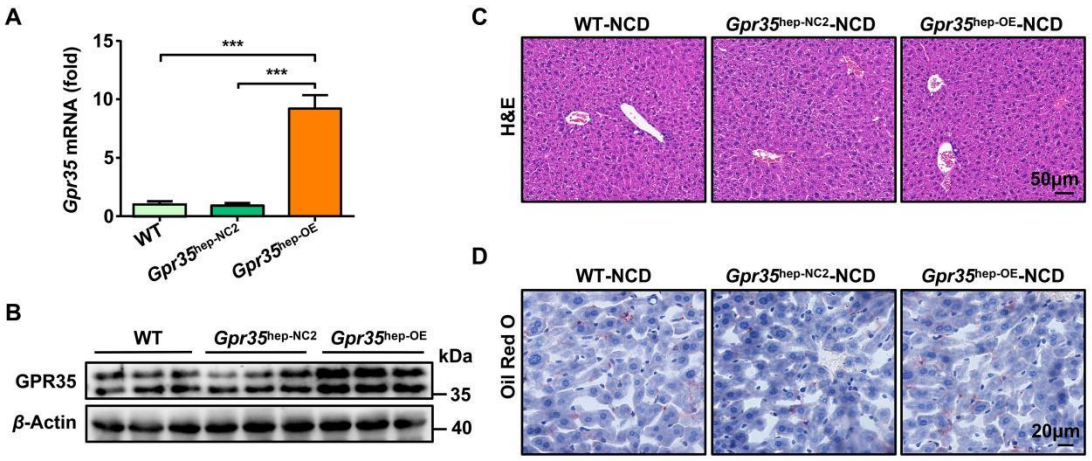

Figure S4 GPR35 overexpression in hepatocytes (n = 3). C57BL/6J mice were injected (i.v.) with AAV8-TBG-MCS-EGFP-3Flag-SV40 PolyA(NC) or AAV8-TBG-MCS-*Gpr35*-EGFP-3Flag-SV40 PolyA. Control (*Gpr35*$^{\text{hep-NC2}}$) mice and hepatocyte *Gpr35*-overexpressing (*Gpr35*$^{\text{hep-OE}}$) mice were generated 1 week later. (A) Relative mRNA expression of *Gpr35* in primary hepatocytes. The mRNA expression of genes was normalized to that of *β*-actin. (B) Representative Western blot of GPR35 in primary hepatocytes. (C) H&E staining of liver tissue sections. Scale bar, 50 μm. (D) Oil Red O staining of liver tissue sections. Scale bar, 20 μm. Data are the mean ± SD; ***$P < 0.001$.

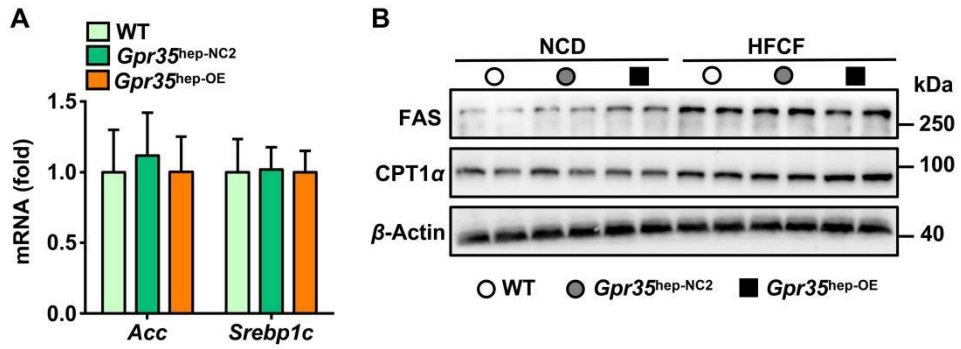

Figure S5 GPR35 overexpression in hepatocytes increases the expression of the genes involved in fatty acid oxidation but not *de novo* lipogenesis in the livers of mice fed the HFCF diet (n = 10). C57BL/6J mice were injected (i.v.) with AAV8-TBG-MCS-EGFP-3Flag-SV40 PolyA(NC) or AAV8-TBG-MCS-*Gpr35*-EGFP-3Flag-SV40 PolyA to generate control (*Gpr35*$^{\text{hep-NC2}}$) mice and hepatocyte *Gpr35*-overexpressing (*Gpr35*$^{\text{hep-OE}}$) mice, which were then fed a NCD or HFCF diet for 16 weeks. (A) Relative mRNA expression of *Acc* and *Srebp1c* in the livers of mice fed the HFCF diet. The mRNA expression of genes was normalized to that of β-actin. (B) Representative Western blot of FAS and CPT1α in the livers of mice fed the NCD or HFCF diet. Data are the mean ± SD.

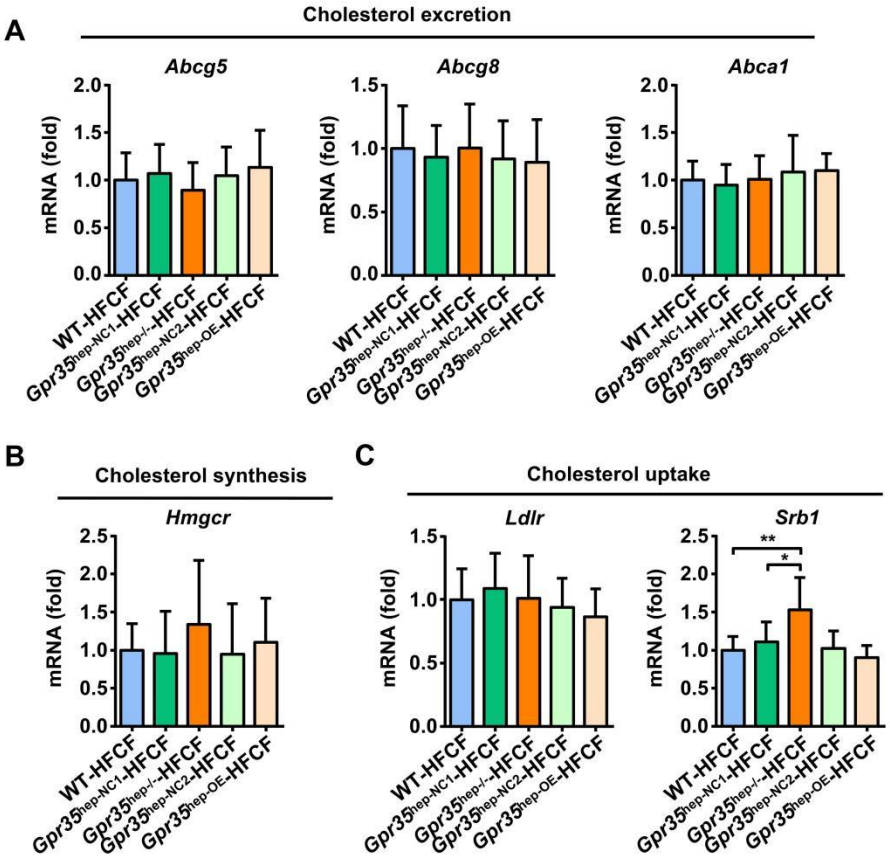

Figure S6 GPR35 expression in hepatocytes does not affect the excretion, synthesis, or uptake of cholesterol in a HFCF diet-induced NASH model (n = 10). WT, *Gpr35*$^{\text{hep-NC1}}$, *Gpr35*$^{\text{hep}-/-}$, *Gpr35*$^{\text{hep-NC2}}$, and *Gpr35*$^{\text{hep-OE}}$ mice were fed a HFCF diet for 16 weeks. Relative mRNA expression of genes involved in the (A) excretion (*Abcg5*, *Abcg8*, *Abca1*), (B) synthesis (*Hmgcr*), and (C) uptake (*Ldlr*, *Srb1*) of cholesterol in the liver. The mRNA expression of genes was normalized to that of β-actin. Data are the mean ± SD.

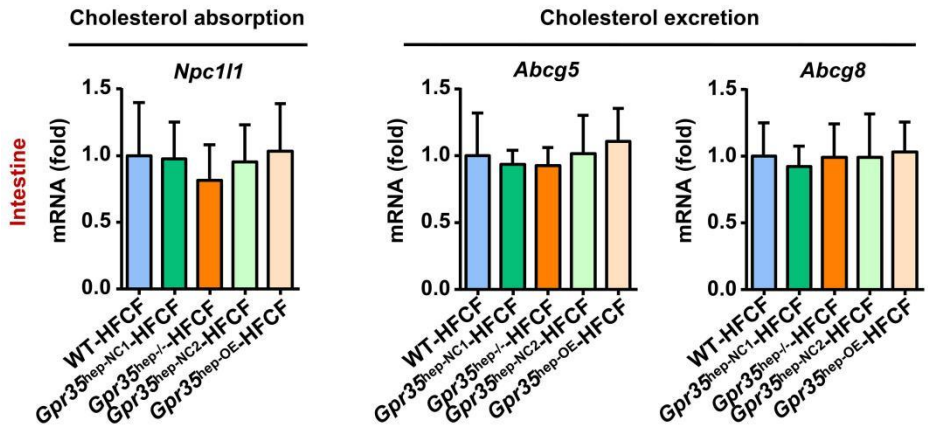

Figure S7 GPR35 expression in hepatocytes does not affect the intestinal absorption and excretion of cholesterol in a HFCF diet-induced NASH model (n = 10). WT, *Gpr35*$^{\text{hep-NC1}}$, *Gpr35*$^{\text{hep}-/-}$, *Gpr35*$^{\text{hep-NC2}}$, and *Gpr35*$^{\text{hep-OE}}$ mice were fed a HFCF diet for 16 weeks. Relative mRNA expression of genes involved in the absorption (*Npc1l1*) and excretion (*Abcg5* and *Abcg8*) of cholesterol in the intestine. The mRNA expression of genes was normalized to that of β-actin. Data are the mean ± SD.

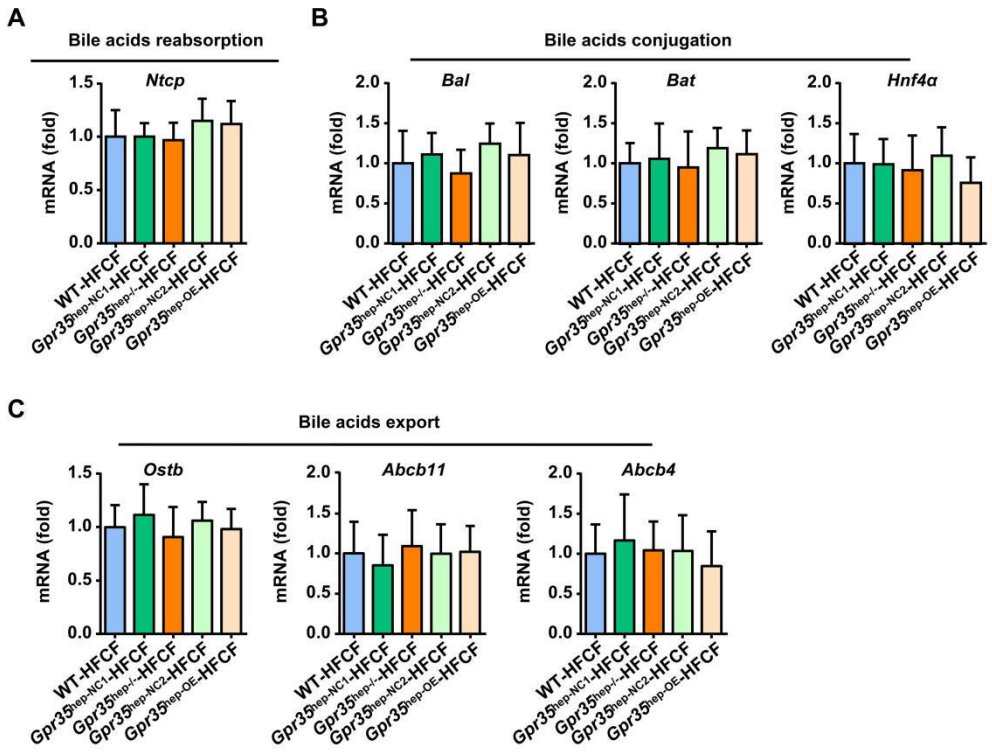

Figure S8 GPR35 expression in hepatocytes does not affect the reabsorption, conjugation, and export of bile acids in the liver in a HFCF diet-induced NASH model (n = 10). WT, *Gpr35*$^{\text{hep-NC1}}$, *Gpr35*$^{\text{hep}-/-}$, *Gpr35*$^{\text{hep-NC2}}$, and *Gpr35*$^{\text{hep-OE}}$ mice were fed a HFCF diet for 16 weeks. Relative mRNA expression of genes involved in the (A) reabsorption (*Ntcp*), (B) conjugation (*Bal*, *Bat*, *Hnf4a1*), and (C) export (*Abcb11*, *Abcb4*, *Ostb*) of bile acids in the liver. The mRNA expression of genes was normalized to that of β-actin. Data are the mean ± SD.

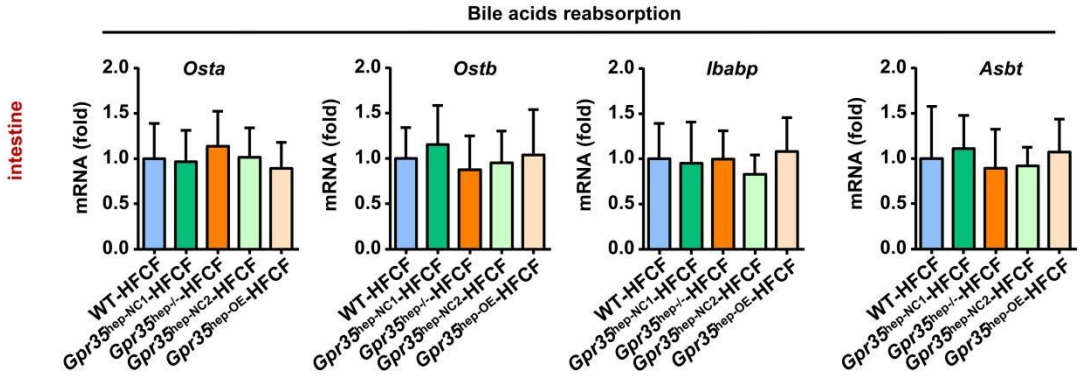

Figure S9 GPR35 expression in hepatocytes does not affect intestinal reabsorption of bile acids in a HFCF diet-induced NASH model (n = 10). WT, *Gpr35*$^{\text{hep-NC1}}$, *Gpr35*$^{\text{hep}-/-}$, *Gpr35*$^{\text{hep-NC2}}$, and *Gpr35*$^{\text{hep-OE}}$ mice were fed a HFCF diet for 16 weeks. Relative mRNA expression of genes involved in the reabsorption (*Osta*, *Ostb*, *Ibabp*, *Asbt*) of bile acids in the intestine. The mRNA expression of genes was normalized to that of β-actin. Data are the mean ± SD.

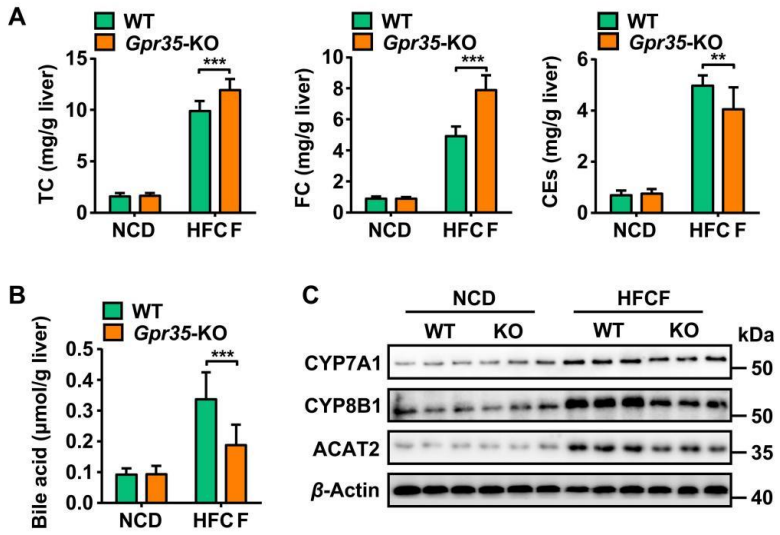

Figure S10 Global deletion of GPR35 prevents ACAT2-mediated cholesterol esterification and CYP7A1-initiated synthesis of bile acids in the livers of HFCF diet-fed mice (n = 6). WT and *Gpr35*-KO mice were fed a NCD or HFCF diet for 16 weeks. (A) TC, FC, and CEs levels in the liver. (B) Bile acid levels in the liver. (C) Representative Western blot of CYP7A1, CYP8B1, and ACAT2 in the liver. Data are the mean ± SD; *$P < 0.05$, **$P < 0.01$, ***$P < 0.001$.

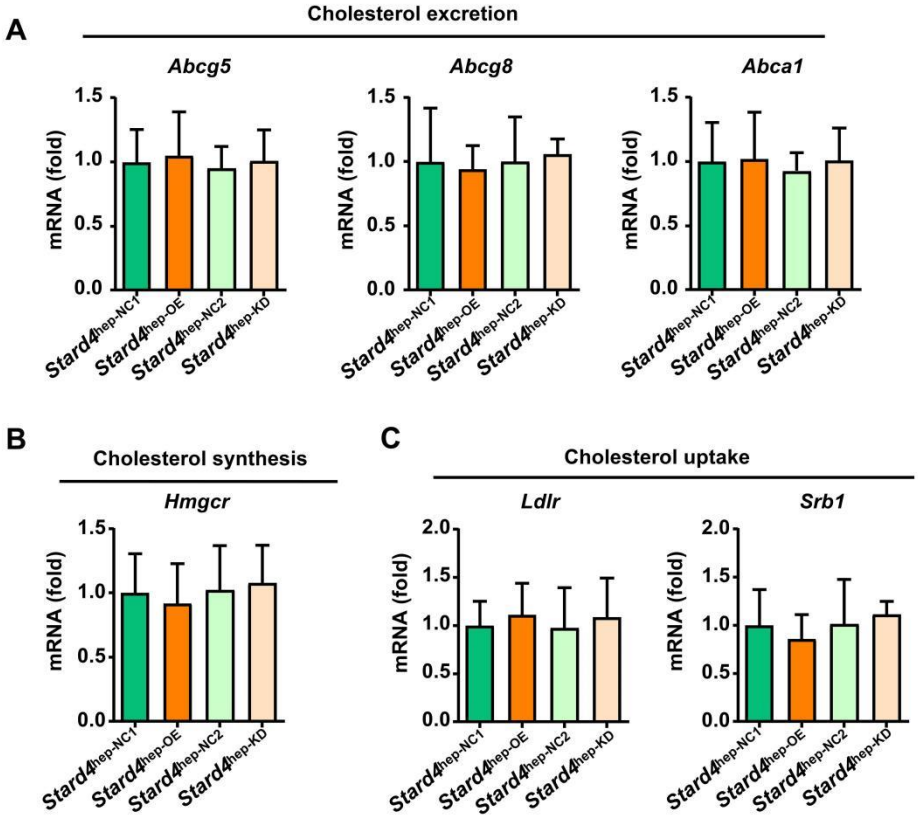

Figure S11 STARD4 does not affect the excretion, synthesis, or uptake of cholesterol in the livers of HFCF diet-fed mice (n = 6). C57BL/6J mice were injected (i.v.) with AAV8-TBG-m-NC-3xFlag-mCherry, AAV8-TBG-m-*Stard4*-3xFlag-mCherry, AV8-TBG-Mir30-m-shRNA(NC)-mCherry or AAV8-TBG-Mir30-m-shRNA(*Stard4*)-mCherry to generate *Stard4*$^{\text{hep-NC1}}$, *Stard4*$^{\text{hep-OE}}$, *Stard4*$^{\text{hep-NC2}}$, and *Stard4*$^{\text{hep-KD}}$ mice, respectively, which were then fed a HFCF diet for 16 weeks. Relative mRNA expression of genes involved in the (A) excretion (*Abcg5*, *Abcg8*, *Abca1*), (B) synthesis (*Hmgcr*), and (C) uptake (*Ldlr*, *Srb1*) of cholesterol in the liver. The mRNA expression of genes was normalized to that of β-actin. Data are the mean ± SD.

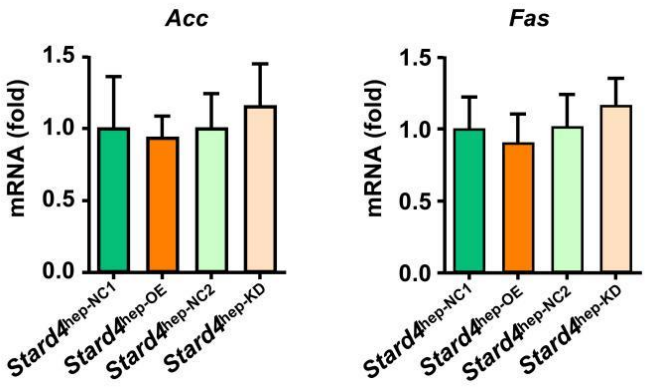

Figure S12 STARD4 does not affect the *de novo* lipogenesis in the livers of HFCF diet-fed mice (n = 6). C57BL/6J mice were injected (i.v.) with AAV8-TBG-m-NC-3xFlag-mCherry, AAV8-TBG-m-*Stard4*-3xFlag-mCherry, AV8-TBG-Mir30-m-shRNA(NC)-mCherry or AAV8-TBG-Mir30-m-shRNA(*Stard4*)-mCherry to generate *Stard4*$^{\text{hep-NC1}}$, *Stard4*$^{\text{hep-OE}}$, *Stard4*$^{\text{hep-NC2}}$, and *Stard4*$^{\text{hep-KD}}$ mice, respectively, which were then fed a HFCF diet for 16 weeks. Relative mRNA expression of genes involved in the de novo lipogenesis (*Acc* and *Fas*) in the liver. The mRNA expression of genes was normalized to that of β-actin. Data are the mean ± SD.

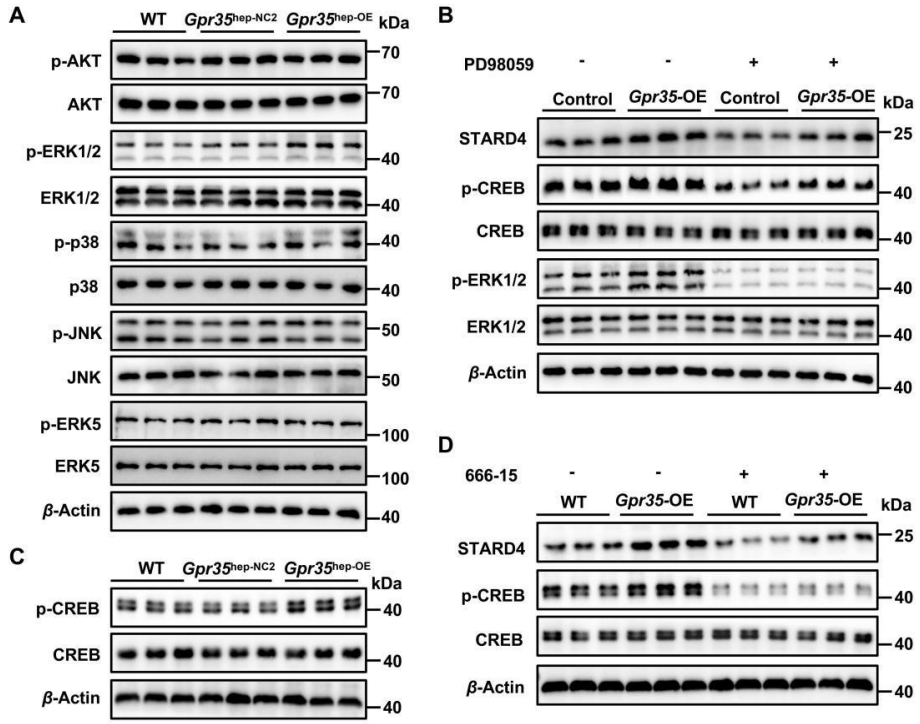

Figure S13 Hepatocyte GPR35 induces STARD4 expression *via* the ERK1/2–CREB signaling pathway. (A) WT, *Gpr35*$^{\text{hep-NC2}}$, and *Gpr35*$^{\text{hep-OE}}$ mice were fed a HFCF diet for 16 weeks. Representative western blot of p-AKT, AKT, p-ERK/2, ERK1/2, p-p38, p38, p-JNK, JNK, p-ERK5 and ERK5 proteins in the liver (n = 10). (B) AML-12 cells were transfected with pEX-3-control or pEX-3-Mus *Gpr35* plasmids using Lipofectamine 2000 to generate control or GPR35-OE cells. GPR35-OE cells were then treated with Kyna (100 μmol/L) to activate GPR35. Representative Western blot of STARD4, p-CREB, CREB, p-ERK1/2 and ERK1/2 in AML-12 cells after PA&OA (0.5 mmol/L/1 mmol/L) treatment for 24 h with or without PD98059 pretreatment (20 μmol/L) for 2 h. (C) WT, *Gpr35*$^{\text{hep-NC2}}$, and *Gpr35*$^{\text{hep-OE}}$ mice were fed a HFCF diet for 16 weeks. Representative Western blot of p-CREB and CREB proteins in the liver (n = 10). (D) AML-12 cells were transfected with pEX-3-control or pEX-3-Mus *Gpr35* plasmids using Lipofectamine 2000 to generate control or GPR35-OE cells. GPR35-OE cells were then treated with Kyna to activate GPR35. Representative Western blot of STARD4, p-CREB, CREB, p-ERK1/2 and ERK1/2 in AML-12 cells after PA/OA (0.5 mmol/L/1 mnol/L) treatment for 24 h with or without 666-15 pretreatment (1 μmol/L) for 2 h. PA, palmitic acid; OA, oleic acid; PD98059, ERK inhibitor; 666-15, CREB inhibitor.

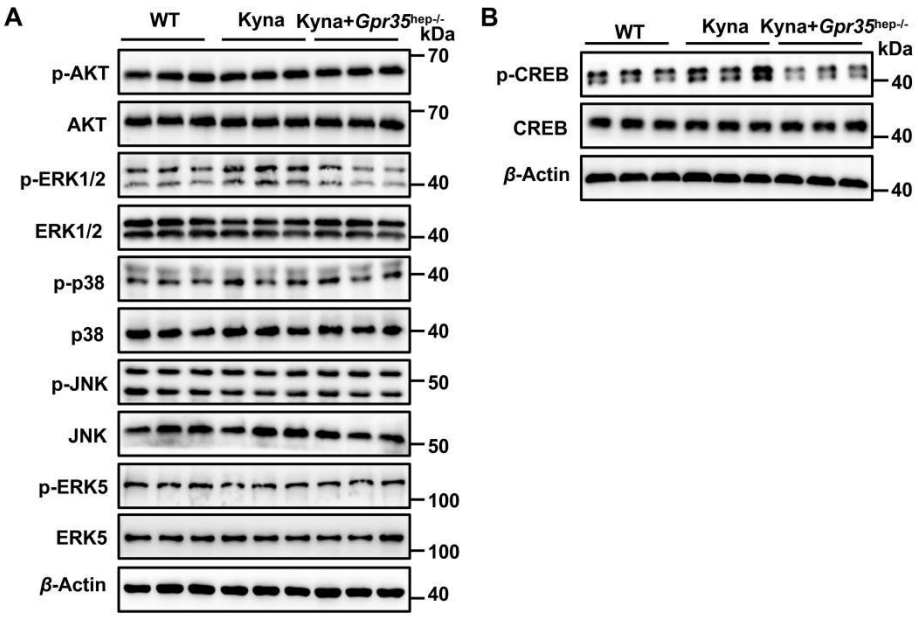

Figure S14 Kyna/GPR35 activates the ERK1/2-CREB signaling pathway in the liver (n = 6). After HFCF-diet feeding for 8 weeks, WT and *Gpr35*$^{hep-/-}$ mice were injected with Kyna (5 mg/kg body weight, i.p.) daily, and HFCF-diet feeding was continued for 8 weeks. (A) Representative western blot of p-AKT, AKT, p-ERK/2, ERK1/2, p-p38, p38, p-JNK, JNK, p-ERK5 and ERK5 proteins in the liver. (B) Representative western blot of p-CREB and CREB proteins in the liver. Kyna, kynurenic acid (an endogenous agonist of GPR35).